AD-A068 475 AIR FORCE HUMAN RESOURCES LAB BROOKS AFB TEX F/G 5/9
ADANCED SIMULATOR FOR PILOT TRAINING (ASPT): G-SEAT OPTIMIZATIO--ETC(U)
FEB 79 D C MCGUIRE, D R LEE

UNCLASSIFIED AFHRL-TR-78-92 NL

| OF |
AD
A068475

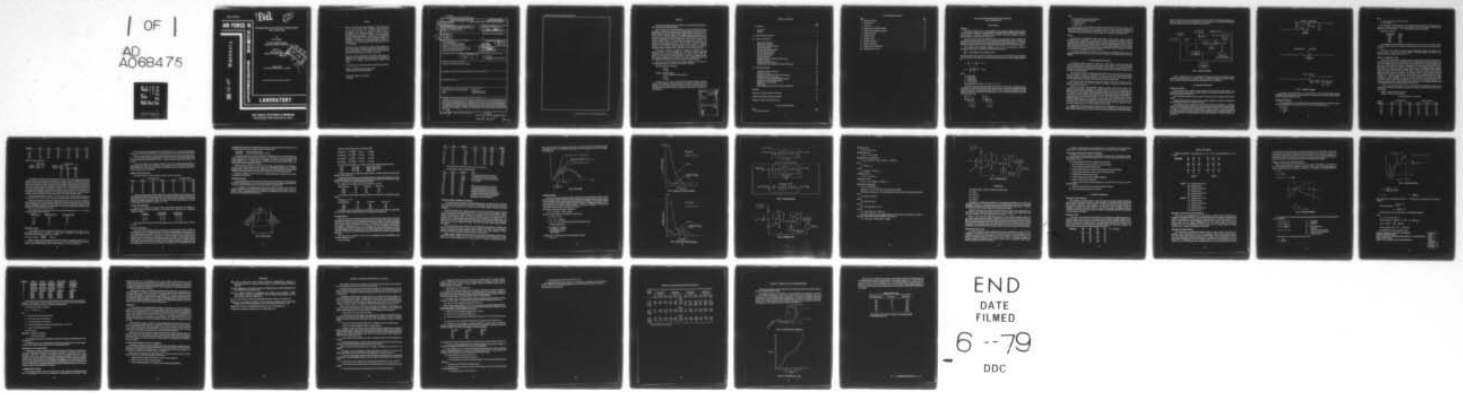

END
DATE
FILMED
6 -79
DDC

AFHRL-TR-78-92

LEVEL II

AIR FORCE HUMAN RESOURCES LABORATORY

ADVANCED SIMULATOR FOR PILOT TRAINING (ASPT): G-SEAT OPTIMIZATION

By

Dan C. McGuire

FLYING TRAINING DIVISION
Williams Air Force Base, Arizona 85224

David R. Lee

Singer-Link Division
Williams Air Force Base, Arizona 85224

February 1979
Interim Report for Period May 1977 – April 1978

AIR FORCE SYSTEMS COMMAND
BROOKS AIR FORCE BASE, TEXAS 78235

NOTICE

When U.S. Government drawings, specifications, or other data are used for any purpose other than a definitely related Government procurement operation, the Government thereby incurs no responsibility nor any obligation whatsoever, and the fact that the Government may have formulated, furnished, or in any way supplied the said drawings, specifications, or other data is not to be regarded by implication or otherwise, as in any manner licensing the holder or any other person or corporation, or conveying any rights or permission to manufacture, use, or sell any patented invention that may in any way be related thereto.

This interim report was submitted by Flying Training Division, Air Force Human Resources Laboratory, Williams Air Force Base, Arizona 85224, under project 1123, with HQ Air Force Human Resources Laboratory (AFSC), Brooks Air Force Base, Texas 78235.

This report has been reviewed by the Information Office (OI) and is releasable to the National Technical Information Service (NTIS). At NTIS, it will be available to the general public, including foreign nations.

This technical report has been reviewed and is approved for publication.

DIRK C. PRATHER, Lieutenant Colonel, USAF
Technical Advisor, Flying Training Division

RONALD W. TERRY, Colonel, USAF
Commander

Unclassified

SECURITY CLASSIFICATION OF THIS PAGE *(When Data Entered)*

REPORT DOCUMENTATION PAGE

READ INSTRUCTIONS BEFORE COMPLETING FORM

1. REPORT NUMBER: AFHRL-TR-78-92	2. GOVT ACCESSION NO.
3. RECIPIENT'S CATALOG NUMBER	
4. TITLE (and Subtitle): ADVANCED SIMULATOR FOR PILOT TRAINING (ASPT): G-SEAT OPTIMIZATION	5. TYPE OF REPORT & PERIOD COVERED: Interim rept. May 77 – Apr 78
6. PERFORMING ORG. REPORT NUMBER	
7. AUTHOR(s): Dan C. McGuire, David R. Lee	8. CONTRACT OR GRANT NUMBER(s)
9. PERFORMING ORGANIZATION NAME AND ADDRESS: Flying Training Division, Air Force Human Resources Laboratory, Williams Air Force Base, Arizona 85224	10. PROGRAM ELEMENT, PROJECT, TASK AREA & WORK UNIT NUMBERS: 62205F, 11231308
11. CONTROLLING OFFICE NAME AND ADDRESS: HQ Air Force Human Resources Laboratory (AFSC), Brooks Air Force Base, Texas 78235	12. REPORT DATE: February 1979
	13. NUMBER OF PAGES: 34
14. MONITORING AGENCY NAME & ADDRESS *(if different from Controlling Office)*	15. SECURITY CLASS. *(of this report)*: Unclassified
	15a. DECLASSIFICATION/DOWNGRADING SCHEDULE

16. DISTRIBUTION STATEMENT *(of this Report)*

Approved for public release; distribution unlimited.

17. DISTRIBUTION STATEMENT *(of the abstract entered in Block 20, if different from Report)*

18. SUPPLEMENTARY NOTES

19. KEY WORDS *(Continue on reverse side if necessary and identify by block number)*

Advanced Simulator for Pilot Training (ASPT)
g-cues
g-seat
haptic system
motion perception system
pneumatic control system

20. ABSTRACT *(Continue on reverse side if necessary and identify by block number)*

This report documents Phase I (of III) of a project to optimize the effectiveness of the ASPT g-seat in terms of both hardware and software performance. The transport lag was reduced to 20 ms by moving the Conoflow valves to the platform and using higher diameter hoses. The time constant was reduced to 150 ms by using larger diameter hoses, changing the needle valve location, and optimizing the settings of the booster and needle valve adjustments. The software has been reorganized, improved, streamlined and documented so that it may be more readily used to determine the most effective drive techniques. The optimized system will be used in a Phase II to determine the most effective drive technique and in a Phase III which will emulate new g-cueing devices, geometries, and drive schemes.

DD FORM 1 JAN 73 1473 EDITION OF 1 NOV 65 IS OBSOLETE

Unclassified

SECURITY CLASSIFICATION OF THIS PAGE *(When Data Entered)*

404 415

PREFACE

This study was conducted in support of project 1123, Flying Training development; task 112310, Simulator Engineering Support.

This is an interim report which covers Phase I of work unit 11231008, ASPT G-seat Optimization. The study was conducted by the Flying Training Division of the Air Force Human Resources Laboratory (AFSC), Williams AFB, Arizona, from summer 1977 to summer 1978. The purpose of Phase I was to establish the nature of the response lags in the g-seat system of the Advanced Simulator for Pilot Training (ASPT) and to minimize the lags by optimizing the hardware configuration and the software execution. The purpose of Phase II will be to determine the most effective drive technique for the optimized ASPT pneumatic g-seat system. Phase III will use the optimized system to emulate new g-cueing devices, geometries, and drive schemes so that a more effective approach can be developed, existing approaches can be compared, and proposed approaches evaluated. Subsequent reports will present the results of Phases II and III.

Appreciation is extended to Singer/Link, in general, and especially to Mr. Jim Sullivan and Mr. Lee Cole, Singer/Link; Mr. Jim Waldrop, Systems Engineering Laboratories; and Mr. Mike Cyrus, AFHRL/FTE, for the time, effort, and advice they devoted to this project; and Ms Stella Southern for cheerful and conscientious typing. The hardware modifications will be installed by Mr. John Archambeault and Mr. Jim Exter, Singer/Link. The figures were drawn by Mr. Dino Campana, Singer/Link.

Due to the extent of hardware and software modifications to be made, the following documentation will be revised upon completion of Phase II:

ASUPT-68 Simulator Test Outline

Vol VII
"G" Seat

ASUPT-74 Simulator Systems
Computer Programs and Documentation

Vol VII
"G" Seat

Although not to be revised, technical report AFHRL-TR-75-59(III), *Advanced Simulation in Undergraduate Pilot Training: G-Seat Development* contains some data and diagrams which may become obsolete. However, the report is still very useful as an introduction to g-seat system design and g-cueing theory and should be reviewed prior to this publication.

TABLE OF CONTENTS

		Page
I.	Introduction	5
	Background	5
	Purpose	6
II.	System Description/Approach	6
III.	Hardware Optimization	7
	Measurement Technique	7
	Pneumatic Hose Diameters	8
	Needle Valve Settings and Location	9
	Reduced Hose Length	10
	Operation Without Booster Valve	11
	Conoflow Valve Adjustments	11
	Booster Valve Adjustments	11
	Operating Pressure Tests	12
	Frequency Response	13
	Analog Input/Output Considerations; D/A Circuits	14
	Feedback Application	15
	Applications to Future Projects	19
	Conclusions/Recommendations for Hardware Configuration	20
IV.	Software Optimization	20
	Explanatory Comment Statements	20
	Reduction of Arrays	20
	Maximization of Linear Flow/Unnecessary Branching	21
	Eliminating Unnecessary Constants	21
	Utilization of Accurate and/or Simplified Techniques	22
	Reorganization in a More Logical Fashion	24
	Applications to Future Projects	24
	Digital Leads	25
	Conclusions/Recommendations for Software Configuration	25
References		26
Appendix A: Conoflow and Booster Valve Setup		27
Appendix B: Hose Diameter Bench Test Results		30
Appendix C: Needle Valve Flow Measurement		31

LIST OF ILLUSTRATIONS

Figure		Page
1	Bench test schematic	7

List of Illustrations (*Continued*)

Figure		Page
2	Strip chart recording	8
3	Inlet of booster	12
4	D/A output	15
5	Pressure cycle with/without feedback	16
6	Exhaust cycle with/without feedback	16
7	Feedback schematic	17
8	Feedback circuit 1	17
9	Feedback circuit 2	19
10	Distortion schematic 1	22
11	Distortion schematic 2	23
C-1	Needle valve flow measurement	31
C-2	Needle valve flow vs turns	31

ADVANCED SIMULATOR FOR PILOT TRAINING (ASPT): G-SEAT OPTIMIZATION

I. INTRODUCTION

Background

The Advanced Simulator for Pilot Training (ASPT) g-seat was delivered to Williams AFB to be used in conjunction with a T-37 simulation. Although designed as a research device with a high degree of flexibility, it was necessary to improve the response time of the system to effectively simulate the g-cues of higher-performance aircraft, such as the A-10 and F-16.

The g-seat Conoflow valves of the ASPT were moved to the motion platform in late 1976/early 1977 to reduce the hose length from 37 feet to 8 feet and thus reduce response time. Tests were conducted to determine the amount of improvement. The results showed that the new transport lag was .37 to .41 of the old transport lag, and the new time constant (time to 63% of final value) was .8 of the old time constant.

From Truxal's Control Engineer's Handbook, 1958, p. 16–11, the transport lag should be proportional to line length, and the time constant should be proportional to

$\frac{L^2}{D^2}$ (L = line length; D = inside diameter of hose).

When the Conoflow valves were moved to the platform, the hose size was reduced (due to space limitations) from 0.375-inch i.d. to 0.250-inch i.d. The theoretical improvements due to reduced line length should then be

$$t_2 = \frac{L_2}{L_1} \quad t_1 = \frac{8}{37} t_1 = .22\, t_1$$

$$T_2 = \frac{L_2^2 \quad D_1^2 \quad T_1}{D_2^2 \quad L_1^2} = .11\, T_1$$

where

t = transport lag
T = time constant
L = length of hose
D = inside diameter

From tests (McGuire, 1977): $t_2 = .37$ to $.41\, t_1$; $T_2 = .8\, T_1$

The difference between the theoretical and actual improvement in time constant would be due to the contributions of lag within the Conoflow valve, booster valves and g-seat bellow assemblies (assuming accuracy with respect to predicted hose change effects). In order to reconcile the differences, the g-seat bellows, Conoflow valve, and booster valve would need to account for 78% of the total time constant and 23% of the transport lag.

$B + L = T$	$B + L = t$
$B + .11\, L = .8\, T$	$B + .22L = .4\, t$
$.89\, L = .2\, T$	$.78\, L = .6\, t$
$L = .22\, T$	$L = .77\, t$
$B = .78\, T$	$B = .23\, t$

where

B = bellow and valves time delay contributions
L = hose length time delay contribution
T = total time constant
t = transport lag

It was not clear, however, whether the difference between theoretical and actual was due to the bellow/valves delay time contribution, the hose diameter change having more impact than predicted, the mathematical model being incorrect, the assumptions violated, or an unknown parameter involvement. It was also believed that more improvements could be made to other components of the g-seat system.

Purpose

At this point, it was decided to build a g-seat bench test rig in order to conduct a conclusive investigation into the optimization of the various g-seat hardware components. This includes the effect of hose inside diameters, needle valve settings and location, Conoflow valve adjustments, reduced hose lengths, operating pressures, digital to analog (D/A) circuit modifications, feedback application, and booster valve adjustments. Software optimization was also planned, to include adding explanatory comments, reducing arrays, maximizing linear flow, eliminating unnecessary branching and constants, utilizing more effective, faster techniques and reorganizing in a more logical fashion.

The software optimization will result in a more usable and understandable program which will facilitate determining the most effective drive techniques under Phase II and using auxiliary devices under Phase III.

II. SYSTEM DESCRIPTION/APPROACH

The ASPT g-seat system consists of a seatpan with 16 active bellows, a backrest with nine active bellows, thigh panels with six active cells, and an active seat belt. Each of the 32 items is individually controlled via pneumatic hoses leading from the pneumatic control package to the seat elements. The 32 pneumatic control devices are in turn governed in open-loop fashion by computer linkage operating under the control of the g-seat software.

The fundamental premise in designing the g-seat operation is the concept that aircraft acceleration equals seat position. In general, the seat should "fall away" from the areas of increased flesh pressure normally resulting from seat/subject acceleration. An exception to this rule is the contouring concept wherein localized areas of back and buttocks are subjected to increased flesh pressure.

The lap belt actuator, six thigh panel air cells, nine backrest air cells, and 16 seatpan air cells are treated as excursion devices. The amount of excursion is controlled by the pressure of air delivered to the device and the load on the device.

Thirty-two low-pressure electro-pneumatic transducers (Conoflow valves) form the heart of the pneumatic control package. Compressed air at 25 psig is supplied to each of the 32 transducers. The pressure of the air output by each transducer varies linearly with the current of the control signal applied to the transducer. The control signal is produced through D/A linkages interfacing the control package with the computer software responsible for g-seat control. To insure rapid exhaust cycle time, each transducer is equipped with a one-to-one pneumatic booster valve relay. The exhaust capability of the booster is considerably higher than that of the transducer, and the presence of the relay between air cell and transducer tends to dampen pressure oscillations. A needle valve is located between the Conoflow valve and the booster valve in order to accomplish exhaust commands quickly and, more importantly, reduce hysteresis. Transfer functions can be found in Albery and Hunter (1978).

A g-seat bench test rig was constructed in order to conduct the investigation into optimization of the g-seat hardware components. The bench test consisted of an air compressor, pneumatic hoses, regulator valve, Conoflow valve, needle valve, booster valve, instrumented (potentiometer, accelerometer) bellow

with lead weights, strip chart recorder, signal generator, and voltmeter. The configuration duplicated the ASPT g-seat system as much as possible (Figure 1). Each component of the test rig could be adjusted, removed, or replaced and the effect on bellow response recorded.

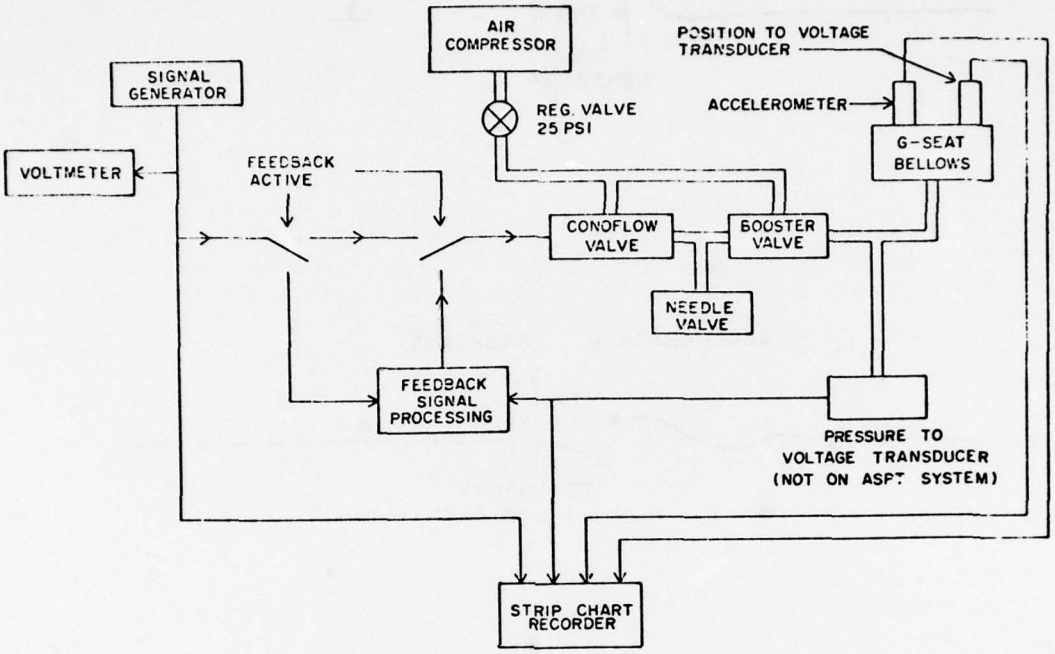

Figure 1. **Bench test schematic.**

Software optimization was to be accomplished by analysis of each step of the existing program to identify areas needing explanatory comments, areas of unnecessary branching and constants, excessive arrays, improvable techniques and areas needing reorganization into a more logical form.

III. HARDWARE OPTIMIZATION

Measurement Technique

The strip chart output consisted of three channels: (a) the input voltage signal applied to the Conoflow valve, (b) the output of a potentiometer attached to the g-seat bellows, and (c) the output of an accelerometer attached to the bellows.

Two items were considered important enough to measure for each test: transport lag time and time constant.

Transport lag time is the time required to begin a response, measured from application of the signal to the first noticeable response of the accelerometer tracing.

Time constant is the time required for the response to reach 63% of the final value $(1 - \frac{1}{e})$. This was measured on the potentiometer trace from the point of acceleration response to the 63% value. See Figure 2 for a strip chart recording example. Another measurement of interest was rise time, the time required for the response to rise from 10% to 90% of its final value. A response could have a very good time constant but a poor rise time due to a quick excursion to 63% of the final value but a much slower approach to the final value. Rise time was usually measured only when visually significant by a tendency to "glide" to a final value.

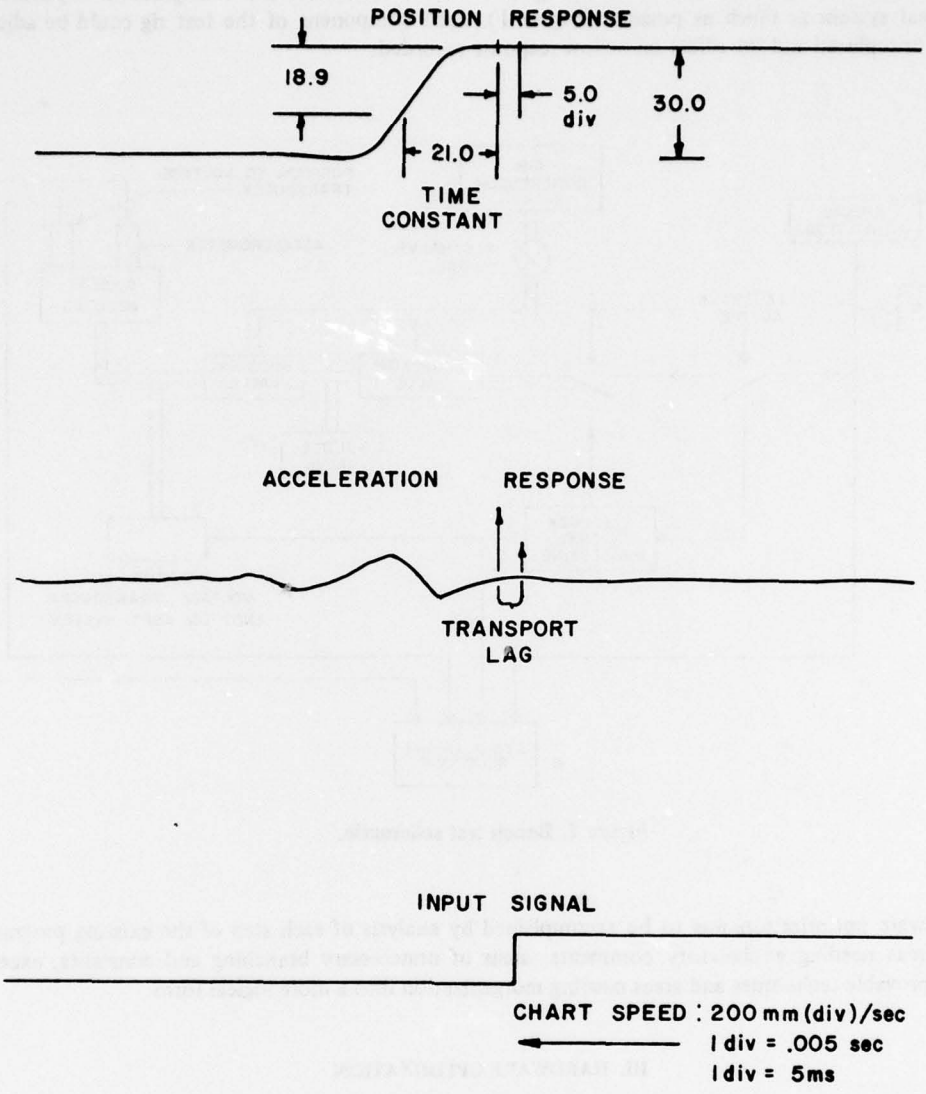

Figure 2. **Strip chart recording.**

In addition to these measurements, it was also important to note exceptionally large overshoots, oscillations and discontinuities in the response trace which would render the system unacceptable regardless of the characteristic measurements above.

Pneumatic Hose Diameters

The first investigation was to determine the effect of hose inside diameter on the bellow response time. Four hose sizes were used: 0.400, 0.375, 0.250, and 0.1875 inch (inside diameter).

From Truxal,

$$\tau_2 = \left(\frac{D_1^2}{D_2^2}\right)\tau_1$$

where

τ = time constant (time to 63% of final value)
D = inside diameter

Thus increasing the inside diameter of the pneumatic hoses should improve (decrease) the time constant of the bellow response. The time constants presented below are the average of the inflation and exhaust cycle time constants (for a −7 to −3 V command, from chart in Appendix B).

Using 0.1875 as the base:

Hose Size (in)	τ (ms)
0.1875	318.8
0.250	156.3
0.375	111.3
0.400	98.8

The discrepancy between theoretical and actual values can be accounted for by Conoflow, bellow, and booster contributions, hose size estimation, measurement errors, and the effect of needle valve use (set at 5/8 turn).

However, the results clearly show that the largest possible inside diameter hoses should be used whenever possible. A change from 0.250-inch diameter to 0.400-inch diameter will yield a 58 ms improvement in time constant for steps of −3 to −7 V.

Needle Valve Settings and Location

During ASPT hardware/software integration testing, a striking difference between the operation of the various Conoflow valves was noticed by Kron (1977). Some displayed small pressure hysteresis (1/4 psi) while others displayed more than double this value. The latter also seemed to require considerably more time to arrive at commanded lower pressures. Examination of the Conoflow valves revealed that the better performing valves were poorly constructed in the diaphragm area. The diaphragm contains an exhaust orifice which, if perfectly assembled, *is co-planar* with the poppet valve plunger located immediately beneath the exhaust orifice cone. During the final stages of an exhaust command, the orifice meets the plunger and tends to ride above the plunger on an "inverse air cushion." Poorly constructed valves with slightly distorted diaphragms did not permit the exhaust orifice cone to approach the plunger in a coplanar condition. As a result, scavenged air flow was increased, exhaust commands were more quickly accomplished, and more importantly, hysteresis was lowered. The solution was to equip each valve with a needle bleed which would effectively duplicate the "offset" air flow condition displayed by the non-coplanar valves and force a prompt seating of the exhaust orifice cone on the plunger head. The needle valve was intalled between the Conoflow valve and the booster valve.

In order to gain experience with the use of the needle valves, an investigation was made into the effects of various needle valve settings and the addition of a needle valve between the booster valve and the g-seat bellows.

Needle A: Between Conoflow and booster
Needle B: Between booster and bellow

Bellow with weight of 5.3 lb attached

(Turns)	Up to Down (ms)			Down to Up (ms)		
Needle A	Tran	Tau	Total	Tran	Tau	Total
0	20	105	125	20	137	157
1/8	20	107	127	17	135	152
1/4	20	107	127	20	135	155
3/8	20	105	125	20	137	157
1/2	20	107	127	20	135	155
1	17	100	117	20	132	152

Needle B	Tran	Tau	Total	Tran	Tau	Total
0	20	105	125	20	137	157
1/8	20	110	130	20	130	150
1/4	15	117	132	20	130	150
5/16	20	112	132	20	130	150
3/8	17.5	110	127	20	125	145

Without a weight on the bellow:

	Up to Down			Down to Up		
Needle A:	Total:	116	Needle A:	Total:	152	
Needle B:	Total:	122	Needle B:	Tran	Tau	Total
				20	140	160
				20	122	142
				20	115	135
				20	102	122
				15	110	125

The results show that there is not much difference between needle valve locations (A vs. B) by time constants. However, close examination of the strip chart recording reveals that a needle valve between the booster and bellow (needle B) can control the amount of overshoot and the slow glide to the final value of bellow excursions. Without a weight on the bellows, needle B also can significantly reduce response time for down-to-up excursions; this would be applicable to backrest bellows or peripheral seatpan cells which do not support much pilot weight. It would thus be desirable to place a needle valve after the output of the booster valve. Space limitations and compressor load will not permit the inclusion of two needle valves. As the needle valve was originally installed to reduce hysteresis, if alternative means to reduce hysteresis is feasible, the needle valves should be moved from the input to the output of the booster valves.

The needle bleed should not exceed 3 to 4 in^3/sec due to pump capacity. This corresponds to a needle setting of 3/8 to 1/4 turn. The procedure used to establish this flow rate is described in Appendix C.

Based on these results, the setting of the needle valve should be at 1/8 to 3/16 turn. At this setting, there is a sharper arrival at the final excursion values and a time constant improvement. The trade-off is in excursion magnitude. The needle valve seems to delete that portion of excursion where the glide normally appears. This magnitude degradation can be compensated by increasing commands as the needle valve effect is constant over the range of normal commands.

The following pressure ranges were measured with needle valve adjustments for a –7 to –3 V square wave signal (needle at output of booster):

Needle (turns)	High Pressure (psig)	Low Pressure (psig)
0	4.3	2.1
1/8	4.0	2.0
1/4	3.7	1.8
5/16	3.6	1.7
3/8	3.6	1.6

Reduced Hose Length

It was suggested by Cyrus and Makinney (1976) that shorter hose lengths from Conoflow valve to seat bellows would provide a reduction in transport lag. The magnitude of improvement can be theoretically derived from the speed of sound: 1116 ft/sec.

Time to travel one foot: $\frac{1 \text{ ft sec}}{1{,}100 \text{ ft}}$ .89 ms/ft

Thus for 37 feet of hose line, the transport lag for the hose pressure propagation should be .89 x 37 = 33 ms. The Cyrus/Makinney tests yielded a transport lag of 45 to 50 ms. This would indicate that the Conoflow, booster, and g-seat bellow contributed the remaining 12 to 17 ms of transport lag.

For the 8-foot hose, the transport lag for the line should be .89 x 8 = 7 ms. The bench tests showed a transport lag of 20 ms, which would leave 13 ms contributed by the Conoflow, booster, and g-seat bellows.

Thus the Conoflow, booster, and g-seat bellows assembly has a total transport lag of approximately 12 to 13 ms. The 8-foot hose has approximately 7 ms of lag and the 37-foot hose approximately 33 ms. The transport lag improvement was then 26 ms (33 – 7 ms), a total transport improvement of 55% to 60% (26/50).

From Truxal (1958), the time constant contribution from the hose length change should only be approximately 3 ms, which would correspond to no noticeable effect for the bench tests. The previous ASPT tests (McGuire, 1977) show a time constant improvement but this was probably actually due to different needle or booster valve settings.

Operation Without Booster Valve

The booster valve was removed to determine the effect on system performance.

	Up to Down (ms)			Down to Up (ms)		
Needle	Trans	Tau	Total	Trans	Tau	Total
0	20	241	264	12	88	100
1/8	16	210	236	12	88	100
1/4	16	192	208	12	88	100
5/16	20	176	196	12	88	100
3/8	12	184	196	12	88	100
1/2	16	172	188	12	88	100

Although these data appear relatively stable, the strip chart recordings show some overshoot at low needle valve settings, large overshoots at higher needle valve settings, and extreme exhaust cycle oscillations. Thus, although it is possible to operate without the booster valve, the effect is unacceptable. The excursion magnitude was slightly increased upon booster valve removal, but the above data were taken for a 1-inch excursion range, which is equivalent to a normal –7 to –3 V.

Conoflow Valve Adjustments

There are two controls on the Conoflow valve: the range select switch and a screw adjustment. A calibration procedure is located in Appendix A. The effects of the "range select" for a voltage step command are as follows:

Range Select	–2 to –8 V Pressure Range	–3 to –7 V Pressure Range
1 – 5	1.3 – 4.3	1.8 – 3.8
4 – 20	.75 – 1.6	.9 – 1.5
10 – 50	.6 – .9	.7 – .85

Screw adjustment for range raises or lowers the high point and to a lesser degree raises or lowers the low point.

Booster Valve Adjustments

The booster screw adjustment cannot be described by a table of transport and time constants for various signals. Its effect is very highly dependent on the needle valve setting and the operating pressure. As the operating pressure is increased, the booster valve becomes unstable (vibrates, loud noise) unless the booster screw and/or needle valve is opened more. As the screw is opened, though, the performance is degraded in terms of time constant and smoothness of response. In addition, as the needle valve is opened, the normal effect of the needle occurs: the needle valve tends to remove that portion of "gliding" excursion which yields a bad rise time. After the excursion is reduced, additional needle valve opening tends to take the remaining glide from the inflating cycle and place it on the exhaust cycle. The needle valve also affects

the stability of the booster valve. The three items, booster screw, operating pressure, and needle valve, were iteratively adjusted several times, yielding an optimum configuration of:

booster screw: 1/4 turn CCW from closed
needle valve: 3/16 turn CCW from closed for 15 psig

It is suspected that the booster screw adjustment is responsible for much of the discrepancies and poor response in previous testing. Each booster valve screw was probably turned until it became stable without adjustment to the needle valve or considering the effect on system performance. The recommendation, then, is to make all adjustments accessible upon moving the Conoflow valves to the platform and to make the initial settings as above.

Since the pressure needed to be reduced so that the booster valve adjustment can be optimized, a trade-off between reduced pressure for the booster valve and degraded performance due to reduced operating pressure must be made. The booster adjustment has such a dramatic effect that it is believed the degradation from reduced pressure will be more than compensated by the booster valve adjustment.

Booster valve stability can also be improved by applying initial pressure gradually. This can be done automatically with the actuator.

Operating Pressure Tests

It had been shown that in order to make an optimum booster valve adjustment, it would be necessary to reduce the operating pressure. It was then left to determine whether this reduction would degrade any other aspect of system performance and to determine the optimum operating pressure.

If a converging or converging/diverging nozzle shape is assumed for airflow in the booster valve (Figure 3), a graph of flow versus pressure ratio is available to estimate the performance degradations. From Sabersky, Acosta, and Hauptmann (1971), for maximum flow (choked), the ratio of pressure at the exit (Pe) to source pressure (Po) should be less than .53.

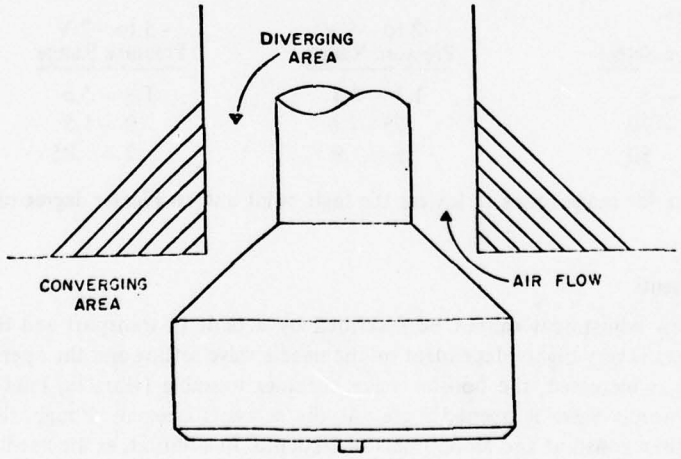

Figure 3. **Inlet of booster.**

Assuming an average bellow pressure of 6 psig (20.7 psia):

For Max Flow: $Po > \frac{20.7}{.53}$ = 39 psia – 24.4 psig

For 99% Max: $Po > \frac{20.7}{.6}$ = 34.5 psia – 19.8 psig

For 95% Max: $Po > \frac{20.7}{.7}$ = 29.6 psia – 14.9 psig

For 90% Max: $Po > \frac{20.7}{.75}$ = 27.4 psia – 12.9 psig

The normal range of pressures is 1 to 10 psig. The range of percentage maximum flow is then:

20 psi	95 to 100%	Median: 98% max flow
15 psi	80 to 100%	Median: 90% max flow
13 psi	60 to 99%	Median: 75%

It would then appear that 15 psig is the optimum pressure to maintain maximum flow and decrease instability of the booster valve.

A larger g-seat bellow weight was used to determine whether an unacceptable degradation would exist for cells under higher loads (tuberosities). The cells typically under higher loads require higher average pressure to compensate so that a greater degradation was expected.

For a weight of 15 lb, average pressure of 6 psig, voltage step –2 to +2 V:

Operating Pressure	Trans	Up to Down	Down to Up
15 psi	20	110	145
20 psi	20	110	143
25 psi	20	110	143

A test with the normal 5-lb load was made to verify that 15 psig would be an acceptable operating pressure.

Voltage step –7 to –3 V

Operating Pressure	Trans	Up to Down	Down to Up
15 psi	20	100	120
20 psi	20	100	120
20 psi	20	100	115

The booster screw and needle valve had very little effect with the larger weight. The larger weight tends to inhibit the "glide" previously exhibited and compensated by the needle valve.

Frequency Response

With a sine wave input, time delay measurements were taken for frequencies from .001 to 4 Hz. Time differences were measured from a mean input signal voltage and a neutral cell excursion point to determine time lag between signal and excursion mean points. By conversion of divisions read on the recording strip chart to time in seconds and multiplying this time lag by 2 π frequency, the lag angle for each frequency was computed. A voltage range of –8 to –2 V was used so that a direct comparison with the previous Cyrus-Makinney tests would be possible (1976). Two weights were used since the booster screw could be closed more (slightly improving the performance) with a higher weight without losing stability and a higher load than 5 lb will occur on the ASPT g-seat, especially on the bellows directly below the pilot's ischial tuberosities.

The results show a bandpass of at least .3 Hz; the unoptimized system (Cyrus/Makinney tests) exhibited a bandpass of .7 Hz.

With 5.3-lb weight:

Hz	Mag	Decibels	Div	Sec	Rad	Degrees
.05	41	0	N/A[a]	N/A[a]	N/A[a]	N/A[a]
.1	40	−.214	N/A[a]	N/A[a]	N/A[a]	N/A[a]
1.0	31	−2.43	27	.135	.85	48.7
1.5	30	−2.71	24	.120	1.13	64.7
2.0	30	−2.71	22	.110	1.38	79.1
2.5	31	−2.43	21	.105	1.65	94.5
3.0	29	−3.01	21.5	.107	2.02	115.7
3.3	27	−3.63	22	.110	2.42	138.7
4.0	20.5	−6.02	22	.110	2.74	157.0

[a]At low frequencies, the potentiometer would stick, causing erroneous data.

With 10-lb weight: (booster readjusted slightly)

Hz	Mag	Decibels	Notes
.001	46.5	0	Chart needle lost 20% of the input signal, so probably also lost 20% of potentiometer data. (Therefore, increase these data by 25% to compensate).
.01	45.5	−.1888	
.05	44.5	−.3819	
.10	42.0	−.8841	
.50	38.0	−1.75	
1.0	37.5	−1.87	
2.0	39.0	−1.53	When a pressure transducer was connected, the output indicated that momentum was contributing significantly to the bandpass calculated from potentiometer data but this probably occurred in the previous unoptimized tests as well. That is, both the old and new bandpasses are lower than indicated.
3.0	37.0	−1.99	
3.3	34.0	−2.72	
3.4	32.5	−3.11	
3.5	31.0	−3.52	
4.0	23.0	−6.11	

Analog Input/Output Considerations; D/A Circuits

It was discovered that the ASPT D/A command voltages going to the Conoflow valves were filtered by a circuit with an approximate first order lag of about 0.04 second. This filter was taken out since the g-seat actuators had a response time in excess of this and provided sufficient filtering of D/A signal "stepping."

The ASPT A/D filters, with a first-order time lag of about .005 second, have the purpose of filtering out noise and unwanted inducted signals above 50 Hz. If A/Ds are used to monitor pressure or position response of the actuators, these filters would have to be considered, or taken out. If they were taken out, however, the high frequency noise on the A/D line would be converted by the sampling rate to low frequency noise. A better approach would probably be to leave the filters in place and use a first order digital lead to correct for the small A/D filter lag. This should be fairly accurate at a 60 Hz sample rate, since the g-seat actuator response lag is above 1/20 second, even with negative pressure feedback enhancement.

Also to be taken into account is the delay due to the analog input/output (I/O) rate. This delay is the period of time between pilot input and the cue output command to the actuator. This can probably be accurately compensated by simply increasing the first order lead on the output commands, if a 30 Hz iteration rate is used (see Operating Pressure Test subsection on digital leads).

Finally, stairstep averaging lag should be taken into account, since its compensation would (as above) simply involve adding a constant to the first order lead. All D/A outputs are in a stairstep form. A first order lag or any other averaging filter (e.g., the g-seat actuator or the human eye perceiving the visual

system), which smooths out the changes in D/A output, has a response which is almost the same as what the response would be to a smooth input which lags the "fresh" D/A outputs by 1/2 of the output update interval (Figure 4).

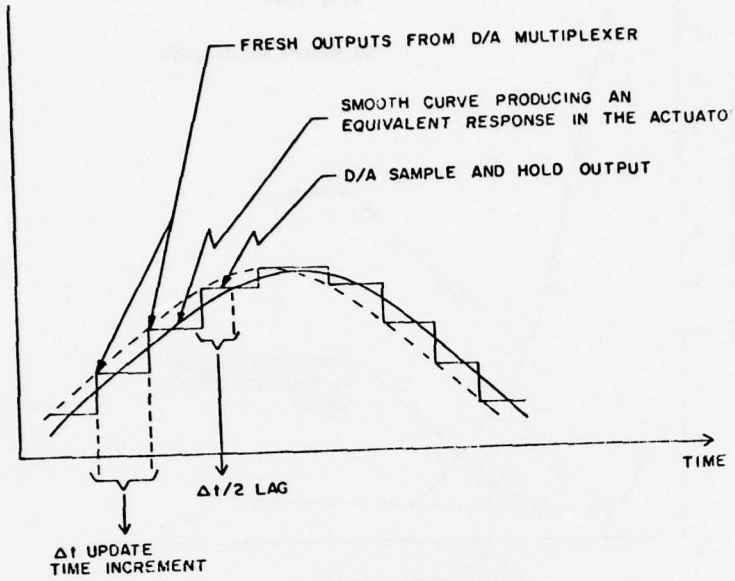

Figure 4. **D/A output.**

Feedback Application

A study of the normal response of the g-seat actuator to step inputs, illustrated in Figures 5 and 6, shows that negative feedback enhancement would be appropriate to investigate. The pressure rate of change of the actuator (in this case, a seat pan bellow) increases rapidly with deviation of the commanded pressure from actual pressure. The negative feedback circuit has the effect of magnifying this deviation by some chosen factor (A). This concept is pictured in Figure 7. Following is a description of the circuit, the equations governing the system, and the results of the study.

The equation governing the electronics of Figure 8 is:

1. $V_I = -R_4 (V_C/R_1 - 20/R_2 + V_P/R_3)$

The other equations which govern the system in steady state are:

2. $P = .475\ V_I + 5.375$
3. $V_I = -V_C$, a constraint
4. $V_P = .31\ P + 3.32$ which is the positive pressure transducer output.*

   P = gauge pressure (psig)

*+10 V applied at + excitation
0 V applied at − excitation
Schaevitz pressure sensor
type P744-002

Amplification of the input signal by (A) is accomplished by making:

5. $R_4/R_1 = A$

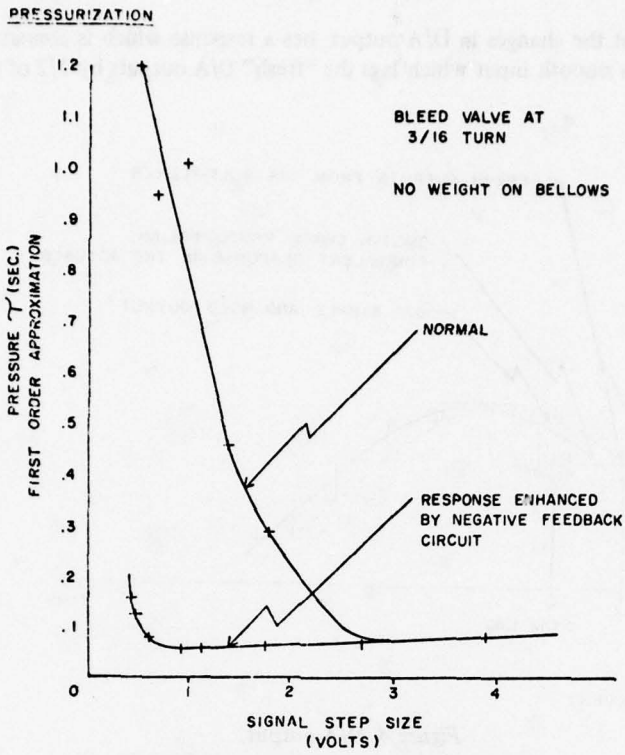

Figure 5. **Pressure cycle with/without feedback.**

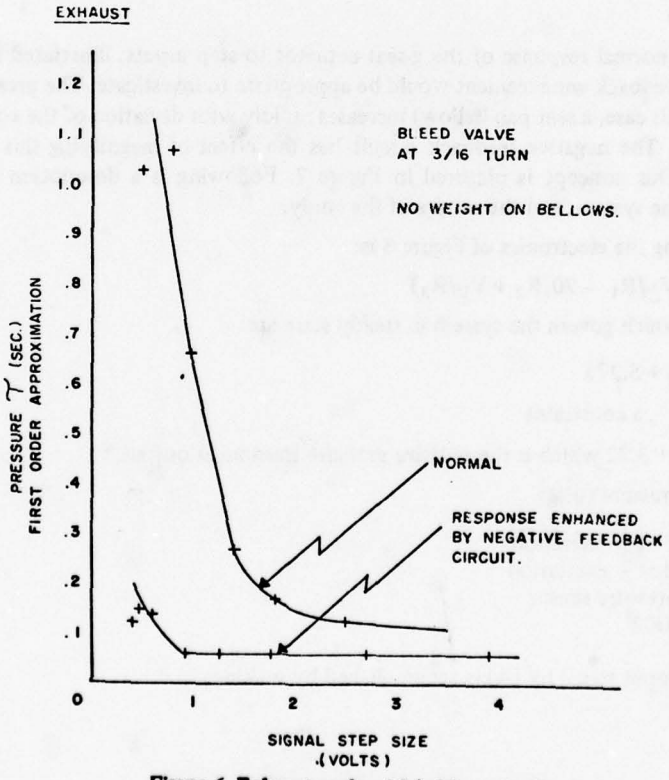

Figure 6. **Exhaust cycle with/without feedback.**

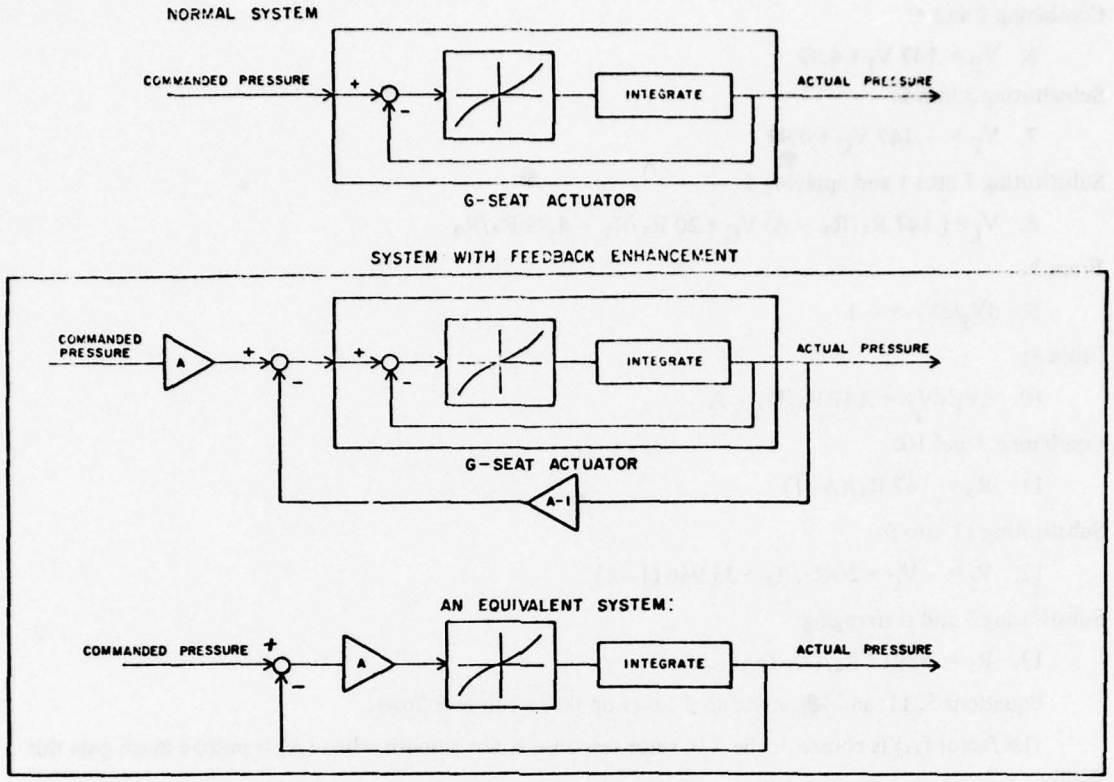

Figure 7. **Feedback schematic.**

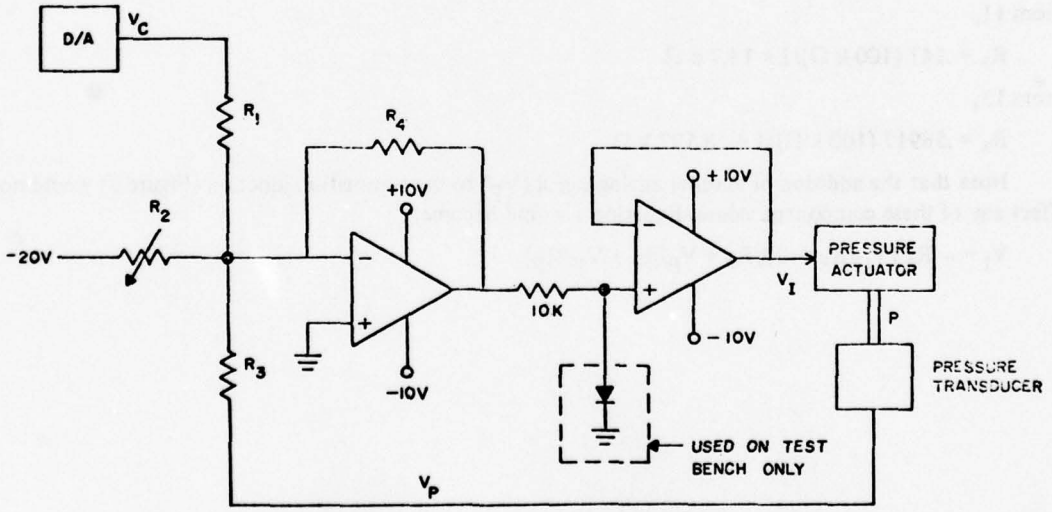

Figure 8. **Feedback circuit 1.**

Combining 2 and 4:

6. $V_P = .147\ V_I + 4.99$

Substituting 3 into 6:

7. $V_P = -.147\ V_C + 4.99$

Substituting 7 into 1 and applying 5:

8. $V_I = (.147\ R_4/R_3 - A)\ V_C + 20\ R_4/R_2 - 4.99\ R_4/R_3$

From 3:

9. $dV_I/dV_C = -1$

From 8:

10. $dV_I/dV_C = .147\ R_4/R_3 - A$

Combining 9 and 10:

11. $R_3 = .147\ R_4/(A-1)$

Substituting 11 into 8:

12. $V_I = -V_C + 20R_4/R_2 + 33.946\ (1-A)$

Substituting 3 and rearranging:

13. $R_2 = .58917\ R_4/(A-1)$

Equations 5, 11, and 13 can be used to set up the circuit as follows:

The factor (A) is chosen to be 2.0, since response is not smooth when (A) is pushed much past this point.

R_4 is chosen to be 100 k Ω

From 5,

$R_1 = 100\ k\ \Omega/2 = 50\ k\ \Omega$

From 11,

$R_3 = .147\ (100\ k\ \Omega)/1 = 14.7\ k\ \Omega$

From 13,

$R_2 = .58917\ (100\ k\ \Omega)/1 = 58.197\ k\ \Omega$

Note that the addition of another analog signal (V_F) to the summation junction (Figure 9) would not effect any of these component values. Equation 1 would become:

$V_I = -R_4\ (V_C/R_1 - 20/R_2 + V_P/R_3 + V_F/R_F)$

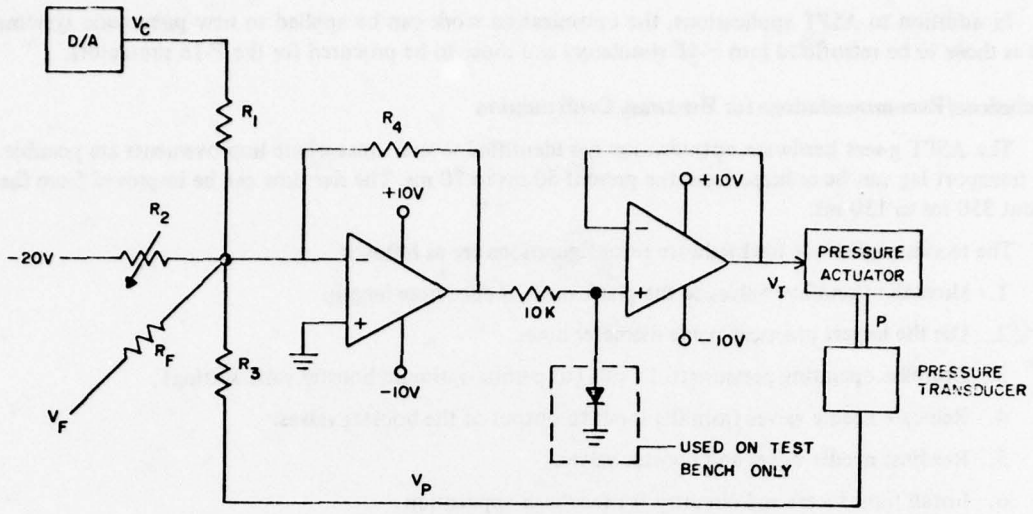

Figure 9. **Feedback circuit 2.**

SYSTEM TEST

The circuit of Figure 7 was set up, using the component values:

$R_1 = 50\ k\ \Omega$

$R_2 = 58.9\ k\ \Omega$

$R_3 = 14.7\ k\ \Omega$

$R_4 = 100\ k\ \Omega$

This makes A = 2. When (A was increased to 3.0, the response of the bellows to a 10 V peak-to-peak triangle wave centered at +5 V (driving V_C) was not smooth. Smoothness decreased further when pressure was applied to the bellows with the hand. Smoothness and stability checked out good with A = 2. This was done with and without the standard weight, and with hand pressure applied.

Response to step inputs was measured with the bleed valve open 3/16 turn. The enhancement circuit was removed and the measurements repeated. Results are shown in Figures 5 and 6. High and low step voltages were actually a very low frequency square wave centered at $-4.\ V(V_1)$.

When A = 3, the lack of smoothness in the response to a slow ramp input is probably caused by the very sudden change in response time (refer to Figures 5 and 6) which occurs as the discrepancy between signal input and actual pressure becomes small. As (A) becomes larger, the sharp bend in the curve shown in Figures 5 and 6 becomes sharper. Given a ramp voltage input, the actuator would hardly respond at all until the pressure error became greater than some value, whereupon the actuator would respond very quickly, overshooting the system back into the slow response portion of the curve, and the cycle would be repeated.

Applications to Future Projects

The ASPT g-seat hardware will be modified into the optimum configuration in summer, 1978. This modification, when combined with the software optimization will permit a detailed investigation into the optimization of software drive philosophies. The more usable software and increased response of the hardware will facilitate attachment of new devices in order to emulate new g-cueing system designs. The improved response and optimized software will be needed in order to adequately simulate higher performance aircraft, such as the A-10 and F-16.

In addition to ASPT applications, the optimization work can be applied to new pneumatic systems such as those to be retrofitted into F-4E simulators and those to be procured for the F-16 simulators.

Conclusions/Recommendations for Hardware Configuration

The ASPT g-seat hardware optimization has identified several areas where improvements are possible. The transport lag can be reduced from the present 50 ms to 20 ms. The rise time can be improved from the present 350 ms to 150 ms.

The recommendations for hardware reconfigurations are as follows:

1. Move the Conoflow valves to the platform to reduce hose length.
2. Use the largest practical inside diameter hoses.
3. Decrease operating pressure to 15 psig (to permit optimum booster valve setting).
4. Relocate needle valves from the input to output of the booster valves.
5. Readjust needle valves and booster valves.
6. Install transducers and circuitry for feedback application.
7. Remove or bypass the D/A circuit filter.
8. Apply a gradual pressure increase technique when the system is first turned on (to prevent booster instability).
9. Check the correct diode values for seatpan and backrest Conoflows.
10. Check the calibration/operation of components.

IV. SOFTWARE OPTIMIZATION

Explanatory Comment Statements

This modification was made in order to document the purpose of the software operations within the software listings. This included identification and/or explanations of the logical variables, computational paths, acceleration distortions, g-suit computations, roll effects, and cell and belt excursions. The cell excursions were divided into seatpan, backrest, and thigh panel which were further divided into translational, contouring, attitude, and roll drive for each of the three axes. The addition of comment statements will make the g-seat program much more usable and understandable and make troubleshooting or software changes more efficient.

Reduction of Arrays

A reduction in arrays was made possible primarily by assuming that the seat will always operate in a symmetric manner. Thus inputs such as contouring schemes, GSERTX, GSERTY, GSERTZ can be completely defined by only one-half of the g-seat cells. Other arrays, such as USECXP (coordinates of cell location in seat frame) were incorporated into other variables since their values would never need to be changed. This reduction in arrays results in less complicated software, less computer core necessary, and faster execution. The inputs for the contouring schemes are as follows:

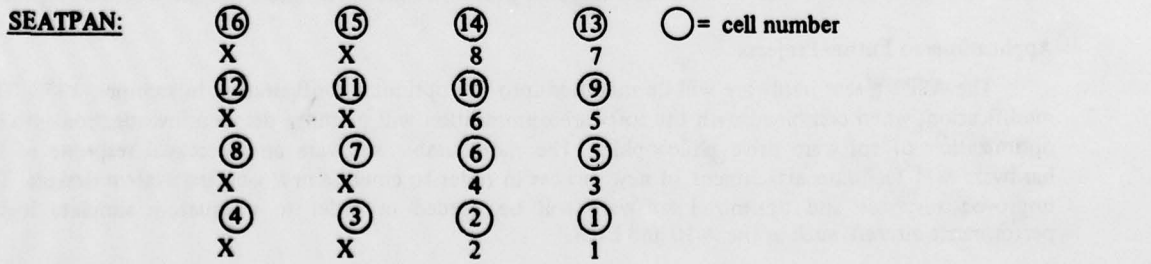

GSERTY AND GSERTZ

GSERTY and GSERTZ 1–8 represents cells 1, 2, 5, 6, 9, 10, 13, 14 and equivalently 4, 3, 8, 7, 12, 11, 16, 15

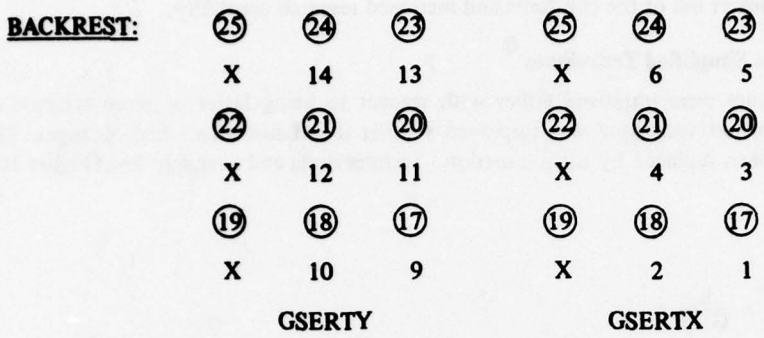

GSERTY (9) represents cell 17 and 19
(10) represents cell 18
(11) represents cell 20 and 22
(12) represents cell 21
(13) represents cell 23 and 25
(14) represents cell 24

GSERTX (1) represents cell 17 and 19
(2) represents cell 18
(3) represents cell 20 and 22
(4) represents cell 21
(5) represents cell 23 and 25
(6) represents cell 24

Maximization of Linear Flow/Unnecessary Branching

The purpose of maximizing linear flow was primarily to reduce confusion. Operations were reorganized or redesigned as necessary to reduce branching and statement numbers. In some instances, the number of programming lines was increased, but overall execution time or confusion was reduced. Several do-loops were replaced by sequential assignment statements which permitted array deletions or more efficient coding. Temporary variables (OTEMP01-16) were used wherever possible for intermediate calculations. The use of the OTEMP array reduced necessary core by reducing variables and reduced execution time by minimizing the duplication of calculations.

Eliminating Unnecessary Constants

The original software contained many instances where two or three constants were used for one application: one for attenuation and one or two for normalization, while only one is actually necessary. The others, while perhaps included for clarity in value derivations, would most likely lead to confusion when trying to change the system performance. Some of the constants were used as multipliers and some as dividers. This was changed so that only one attenuation constant is used. The resulting value for the one attenuator was a very small number which is somewhat clumsy to use in conjunction with the CRT but this

could be alleviated by basing calculations on g-units rather than in/sec^2 units. This reduction in the number of constants used should reduce computer core required, improve execution time, reduce confusion, and make desired changes through the CRT reliable. In a few instances, a new attenuator was generated to separate seatpan and backrest applications. It was felt in these instances that the increase in the number of constants was justified by a clearer use of the constants and increased research capability.

Utilization of Accurate and/or Simplified Techniques

Where possible, techniques were improved either with respect to being faster or more accurate or both. The acceleration distortion technique was improved so that it did not affect high g-ranges. The original distortion logic has been replaced by a combination of a hyperbola and a straight line (Figure 10).

$$L_1 = a.G$$

$$L_2 = c - \frac{h}{G-b}$$

$$L_3 = L_1 + L_2 = c + a.G - \frac{h}{G-b}$$

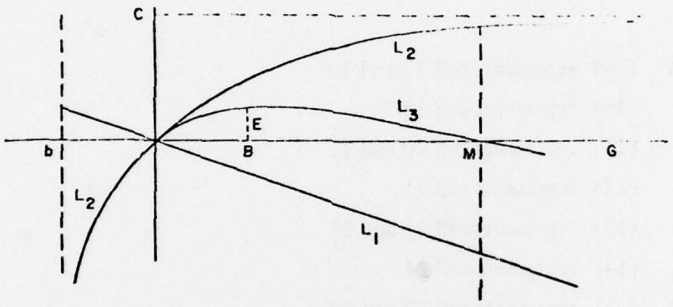

$$L_1 = oG$$

$$L_2 = C - \frac{h}{G-b}$$

$$L_3 = L_1 + L_2 = C + oG - \frac{h}{G-b}$$

Figure 10. **Distortion schematic 1.**

The constants a, b, c, h can be derived by simultaneous equations formed by the following constraints (refer to Figure 11).

1. at $G = B$, $L_3 = E$
2. at $G = M$, $L_3 = 0$
3. at $G = B$, $\frac{dL_3}{dG} = 0$
4. at $G = 0$, $L_3 = 0$

L_1 = straight line
L_2 = hyperbola
L_3 = $L_1 + L_2$
G = input acceleration
T = threshold
B = point of maximum distortion
E = magnitude of max distortion
M = range of distortion

The solutions to b, c, and h are in terms of B, E, and M

$$b = \frac{-B^2}{M.-2B}$$

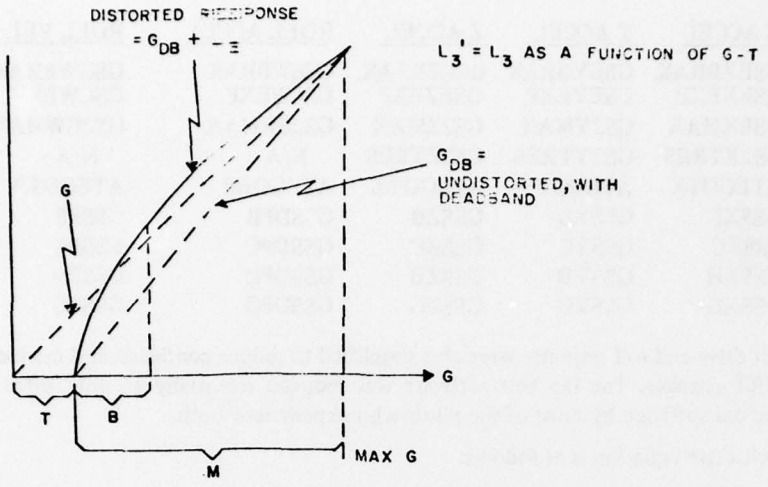

Figure 11. **Distortion schematic 2.**

$$c = \frac{E}{1 + \frac{Bb}{(B-b)^2} + \frac{b}{B-b}}$$

$$h = -cb \qquad a = \frac{-h}{(B-b)^2}$$

After accounting for the threshold (T) effect, ($G - T$ becomes input), the equation of the undistorted response is:

$$\text{Undistorted response} = \frac{M + T}{M}(G - T)$$

$$= (1 + \frac{T}{M})(G - T)$$

Distorted response is obtained by adding L_3' to the undistorted response

where,

$L_3' = L_3$ as a function of $(G - T)$

$$\text{Distorted response} = (1 + \frac{T}{M})(G - T) + a(G - T) + c\ \frac{h}{(G-T)-b}$$

$$\text{Let } g = 1 + \frac{T}{M} + a = 1 + \frac{T}{M} - \frac{h}{(B-b)^2}$$

$$\text{Distorted response} = g(G - T) + c - \frac{h}{(G-T)-b}$$

The FORTRAN code then becomes (for x-axis):

```
GSSXB=-GSEXBRAK**2/(GS2XMAX-2.*GSEXBRAK)
0TEMP01=GSEXBRAK-GSSXB
GSSXC=GSEXEXP/(1.0+GSSXB*GSEXBRAK/0TEMP01**2+GSSXB/0TEMP01)
GSSXH=-GSSXC*GSSXB
GSSXG=1.0+GS2XTRES/GS2XMAX-GSSXH/0TEMP01**2
```

```
ATEGOTX = G
GSSXB = b
GSSXC = c
GSSXH = h
GSSXG = g
GSEXBRAK = B
GSEXEXP = E
GS2XMAX = M
GS2XTRES = T
```

SYMBOL	X ACCEL	Y ACCEL	Z ACCEL	ROLL ACCEL	ROLL VEL
B	GSEXBRAK	GSEYBRAK	GSEZBRAK	GS6WBRAK	GSGWBRAK
E	GSEXEXP	GSEYEXP	GSEZEXP	GS6WEXP	GSGWEXP
M	GSEXMAX	GS2YMAX	GS2ZMAX	GS26WMAX	GS2GWMAX
T	GS2XTRES	GS2YTRES	GS2ZTRES	N/A	N/A
G	ATEGOTX	ATEGOTY	ATEGOTZ	ATEGODP	ATEGOTP
b	GSSXE	GSSYB	GSSZB	GSSDPB	GSSPB
c	GSSXC	GSSYC	GSSZC	GSSDPC	GSSPC
h	GSSXH	GSSYH	GSSZH	GSSDPH	GSSPH
g	GSSXG	GSSYG	GSSZG	GSSDPG	GSSPG

The lap belt drive and roll response were also simplified to reduce confusion and increase reliability of the effects of CRT changes. The lap belt software was reduced essentially to only three lines and was preferred over the old software by most of the pilots who experienced both.

The new belt drive equation is as follows:

$$F = k_z \cdot (Z + 386.) - k_x \cdot X$$

where

F = force of belt over normal buckle-up force

k_z = Z axis response factor and attenuator

k_x = X axis response factor and attenuator

Z = Z accel after deadband and distortion (386 added so that at $-1g$, $F = 0$)

X = X accel after deadband and distortion

The code becomes:

```
ASEFORCE = GSZALTF*AS2ZDELT
         - GSXALTF*AS2XSEAT
```

The intermediate calculations for combining roll response with contouring was simplified without any noticeable effect.

The utilization of better and faster techniques will result in improved execution time easier changes through the CRT, reliable effects of changes, and more understandable variables.

Reorganization in a More Logical Fashion

Reorganization consisted of performing all possible operations in the freeze/reset mode rather than in real time and organizing operations under the components they affected or were related to. Previously, a programmer would need to examine the full listing to insure that a calculation affecting a certain component would not be overlooked (for example the seatpan underlayment drive). The rotational acceleration and rotational velocity computations have been separated. The test mode logic was placed within the freeze mode operations and its use simplified. The capability of the test mode was enhanced to include an input acceleration test mode. The datapool list was alphabetized and only one parameter per line was used to facilitate future changes. Branching was minimized and calculations taken out of do-loops to decrease execution time and readability of the software.

Applications to Future Projects

The software optimization will be very useful in Phase II of the ASPT g-seat optimization. Phase II will be an investigation into the best drive philosophy for applying valid g-cues, especially for high

performance aircraft. The drive philosophies will be varied primarily thorugh CRT inputs and pilot feedback will determine the preferred drives. Each component will be varied, reversed, or increased as necessary. Interactions between components will also need to be examined. The software optimization was a prerequisite for Phase II so that the experimentor could understand what components each parameter would affect and what effect it would have.

This optimization will also have applications in a Phase III which will examine new g-cueing devices or drive philosophies. It is necessary to know how the seat is driven presently in order to identify deficiencies or possible improvements. It was also necessary to understand the exact drive technique so that the software could be adapted to driving accessory equipment which may be attached to the g-cueing system. For example, the thigh cell hoses may be used to drive air pillows placed upon the seatpan. The software which drives the thigh panel would then need to be adapted to the air pillow characteristics. It may even be possible to adapt and/or change the drive through CRT inputs alone.

Digital Leads

The implementation of the negative pressure feedback circuit might permit the approximation (from Figures 5 and 6) that the first order lag in the g-seat actuator is .06 second for exhaust and a straight line function of V_c for pressurization (V_c = rate of change of signal voltage to theConoflow valve). Digital leads based on these approximations break down below about 2 psi per second rate of commanded pressure (estimated from Figures 5 and 6, and the fact that a change of 1 volt in signal voltage produces a .6 psi change in pressure). Thus for slow changes in actuator pressure, there would be errors of up to 0.3 psi uncorrected by digital leads. Of course, more complicated expressions for lead could be derived to improve upon this.

Another approach would be to simply use a first order digital lead which is made to be a function of the rate of change of commanded pressure, to compensate for the lag in the actuator without the addition of the negative feedback circuit. Such leads would, of course, only be accurate if the path of desired actuator rate vs. time could be accurately predicted over each time interval or program iteration. If the path is not smooth and predictable over each time interval, then the lead becomes inaccurate.

Problems arise, therefore, with aircraft angular accelerations which are almost immediate responses to pilot stick inputs (e.g., roll acceleration in response to lateral stick command), which have a maximum frequency of about 5 Hz. If these accelerations are used in determining actuator positions, the digital leads for a 15 Hz calculation rate would be inaccurate. A 30 Hz iteration of the simulation may come close to solving that problem.

Conclusions/Recommendations for Software Configuration

The ASPT g-seat software has been optimized by the addition of explanatory comment statements, reduction of arrays, maximization of linear flow, elimination of unnecessary constants, utilization of faster, more effective techniques, and reorganization into a more logical fashion. This will have applications to drive philosophy investigation and emulation of new g-cueing devices.

There remain a few areas where the ASPT g-seat software could be improved and may be included under the Phase II of the ASPT g-seat optimization. This includes:

1. Changing the input accelerations/attenuators to units of g rather than in/sec^2.
2. Using a software lead factor to improve response.
3. Further simplifications/deletions of capabilities upon identification during Phase II.

REFERENCES

Albery, W.B., & Hunter, E.D. *G-seat component development.* AFHRL-TR-78-18, AD-A055 533. Wright-Patterson AFB, OH: Advanced Systems Division, Air Force Human Resources Laboratory, June 1978.

Cyrus, M., & Makinney, R. *G-seat hardward response tests.* Williams AFB, AZ: Flying Training Division, Air Force Human Resources Laboratory, 1976.

Kron, G.J. *Advanced simulation in undergraduate pilot training: G-seat development.* AFHRL-TR-75-59(III), AD-A017 468. Wright-Patterson AFB, OH: Advanced Systems Division, Air Force Human Resources Laboratory, October 1975.

Kron, G.J. *Needle bleeds on conoflow rack.* Singer SPD Memorandum GJK/77-4, 16 February 1977.

McGuire, D.C. *G-seat hardware performance tests with reduced hose lengths and with needle valves.* Williams AFB, AZ: Flying Training Division, Air Force Human Resources Laboratory, 1977.

Sabersky, R.H., Acosta, A.J., & Hauptmann, E.B. *Fluid flow.* New York: Macmillan, 1971.

Truxal, J.G. *Control engineers' handbook.* New York: McGraw-Hill, 1958.

APPENDIX A: CONOFLOW AND BOOSTER VALVE SETUP

The Conoflow and booster valve components of the g-seat pneumatic drive assembly must be adjusted prior to interfacing these units with the air cells in the g-seat cushion.

The adjustment could be effected at the final bench assembly area with power supplies or after the units are placed in position beside the rear floor joint of the motion base and the D/A's are connected. If the former is used, it is advisable to recheck after installation and D/A hookup to verify the Conoflow valve to D/A interface.

The following procedures describe the setup method for one Conoflow valve/booster assembly. All 31 valves are adjusted in the same manner. The adjustment for the lap belt drive valve is slightly different. The intent of the adjustment is to produce a pressure range of 0 to 12 psi linear as the D/A voltage goes from −10 to +10 V (lap belt valve will be set up for a pressure range of 0 to 15 psi for −10 to +10 V). All the Conoflow valves have a constant −10 V applied to one side so the voltage range is effectively 0 to 20 V.

Note: In that this is likely to be the first time the Conoflow rack assembly is to be pressurized, care must be exercised to get the pressure levels of input air reduced prior to exposure to the Conoflows and booster valves. Therefore, prior to connecting house air or ASPT compressor air to the assembly:

1. Remove caps on T outputs of all booster valves.

2. Disconnect the pneumatic supply line connecting the two Conoflow rack assemblies together. Disconnect at end closest to main regulator. This will permit the regulator to dump to atmospheric pressure. This also protects the C32 valve which does not have a shutoff solenoid between it and supply pressure.

3. Ensure that the shutoff solenoid located next to the regulator is closed: no voltage across it.

4. Unscrew the regulator-adjusting T handle to its highest position.

5. Connect air supply to Conoflow rack and monitor the gauge. If above 30 psi, try screwing T handle on regulator down to reduce to below 30 psi. If below 30 psi or after regulator has been adjusted to below 30 psi, place finger momentarily over tube fitting orfice exposed in (2) above. Watch gauge. Adjust regulator so as to produce 25 psi with this orfice closed. Do not subject shutoff solenoid to pressures in excess of 30 psi for long periods of time.

6. After regulator has been adjusted to provide 25 psi supply, reconnect the hose disconnected in (2) above.

7. When adjusting Conoflows and booster valves it should be remembered that the shutoff solenoid to the bank of valves under adjustment must be opened with 24 Vdc power.

Setup. The following procedures apply after 25 psi supply is established to the valve/booster to be adjusted:

1. Disconnect the air hose leading up to the motion platform manifold at the T output of the booster valve. Replace this with a short length of tubing plugged so as to prevent pressure loss.

2. Connect the pressure gauge provided with each Conoflow rack assembly to the T output fitting on the booster. The pressure gauge is attached to the T at the place normally capped (see (1) under NOTE above).

3. Each Conoflow valve is equipped with an auxilary 1000 Ω potentiometer. Center it for 500 Ω.

4. Each Conoflow valve is equipped with an internal range adjustment potentiometer already in this position.

5. Temporarily disconnect the zener diode shunt from across the Conoflow terminals.

6. Employing a voltage source of known valve and an ammeter, apply 5 V across the Conoflow terminals. Voltage sign can be determined by the pressure gauge. Correct polarity will give a pressure reading. Incorrect polarity will give no pressure reading. Conoflow Corp indicates positive source to terminal #2, negative to terminal #1.

7. Adjust range pot for 1 MA current flow.

8. With 1 MA current flow acting on the unit, adjust zero adjust screw on the front (not inside) of the Conoflow unit to read 3.0 psi on the booster output pressure gauge. It may be necessary to lightly tap (with a pencil etc.) the face of the pressure gauge to obtain a precise reading and zero adjust screw setting. Clockwise (as facing the screw) turns increase pressure; CCW turns decrease pressure.

9. Now apply 20.0 V across the Conoflow terminals, tap gauge face and read pressure. It should read close to 12.0 psi. Adjust to 12.0 psi with the range adjust potentiometer inside the Conoflow unit.

10. Return to 5.0 V and readjust zero adjust screw for 3.0 psi.

Note: If pressure gauge pressure does not seem to decrease when moving from a higher pressure to a lower pressure, suspect the exhaust adjust screw on the face (output side) of the booster. A slight turn CCW should further enlarge the exhaust capability of the booster.

11. Return to 20.0 V and readjust range adjust pot for 12.0 psi.

12. Return to 5.0 V and readjust zero adjust screw.

13. This is an iterative process which should permit 3 psi output at 5.0 V and 12.0 psi output for 20 V.

14. Set voltage to zero, tap gauge face and read pressure. It should reduce to less than 1/4 psi.

15. Finally make a plot of voltage vs. pressure and identify it by valve number. If the pressure transducer is available (one supplied with each set of Conoflow rack assemblies), this should be an easy task with the X-Y plotter. It not, take pressure readings at the following voltages:

0. 0 Volts	2.0 Volts	14.0 Volts
0.2	4.0	16.0
0.4	6.0	18.0
0.6	8.0	20.0
0.8	10.0	
1.0	12.0	

The plot should show linearity between 1.0 and 2.0 V operation with a non-linear "tail off" below 1.0 V.

16. Return to pressure gauge utilization and unhook the plugged piece of hose from the output T of the booster and replace with an air tank sump or spare air bellows assembly.

17. Run voltage up to 20. V across the Conoflow Terminals and then reset voltage to zero (with switch on voltage supply leads, etc.) in step form. Pressure should exhaust to zero immediately and smoothly (no bounce apparent on the pressure gauge needle during the exhaust).

18. Adjust exhaust screw on booster valve so that:

a. There is smooth pressure exhaust (no bounce);

b. The booster does not whistle or sound like a calliope. The only sound should be the hiss of escaping air.

Turning the screw CCW should accomplish the above.

19. Valve C32, the lap belt valve, is set up in the same manner as the other 31 valves except make the following substitutions:

a. Zero adjustment with 4 V and 3 psi, not 5 V.

b. Range adjustment with 20 V and 15 psi, not 12 psi.

20. Replace zener diode before moving on to next valve and run voltage up to 20 V across the Conoflow terminals. Note pressure gauge reading at 20 V, with zene installed, on the plot for this valve.

This completes the setup procedure.

APPENDIX B: HOSE DIAMETER BENCH TEST RESULTS

Hose Dia (in)	Inflation (ms)			Exhaust (ms)			Inflation (ms)			Exhaust (ms)		
	−8 to −2 V			−2 to −8 V			−7 to −3 V			−3 to −7 V		
	Tran	Tau	Total	Tran	Tau	Total	Tran	Tau	Total	Tran	Tau	Total
						25 psi						
0.375	30.0	135.0	165.0	25.0	110.0	135.0	30.0	115.0	145.0	25.0	107.5	132.5
0.250	30.0	187.5	217.5	25.0	180.0	205.0	32.5	147.5	180.0	30.0	165.0	195.0
0.1875	–	–	–	–	–	–	52.5	367.5	420.0	52.5	270.0	322.5
						30 psi						
0.375	27.5	130.0	157.5	30.0	100.0	130.0	27.5	100.0	127.5	30.0	102.5	132.5
0.250	27.5	172.5	200.0	27.5	175.0	202.5	27.5	130.0	157.5	30.0	162.5	192.5
0.1875	–	–	–	–	–	–	–	–	–	–	–	–
						35 psi						
0.375	25.0	125.0	150.0	30.0	102.5	132.5	27.5	102.5	130.0	35.0	100.0	135.0
0.250	35.0	152.5	187.5	40.0	160.0	200.0	40.0	120.0	160.0	30.0	177.5	207.5
0.1875	–	–	–	–	–	–	–	–	–	–	–	–

Note. – Needle valve set at 5/16 turn.

APPENDIX C: NEEDLE VALVE FLOW MEASUREMENT

Following is the procedure used to measure the flow through a needle valve from 0 psig to 6 psig. The needle valve is Skinner Model F221-000.

The measurement setup is shown in Figure C-1. The air was bled from the 6 psig source to an inverted jar, full of water and standing in a disk of water to seal it from the air. For purposes of this rough measurement, the pressure throughout the jar was assumed to be atmospheric. The pressure at the level of the air outlet in the jar was almost exactly atmospheric (Fig C-1). The time (T) for the jar to fill with air (Volume 54.4 in^3) gives a value for the flow of air (W). This measurement was repeated for several needle valve adjustments. The results are shown in the table below and Figure C-2.

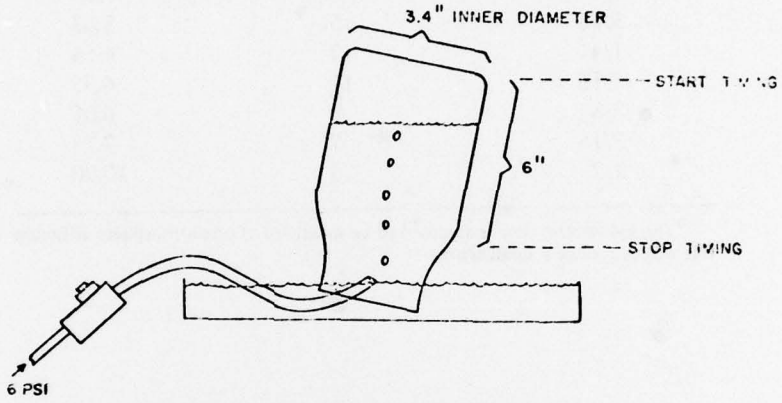

Figure C-1. **Needle valve flow measurement.**

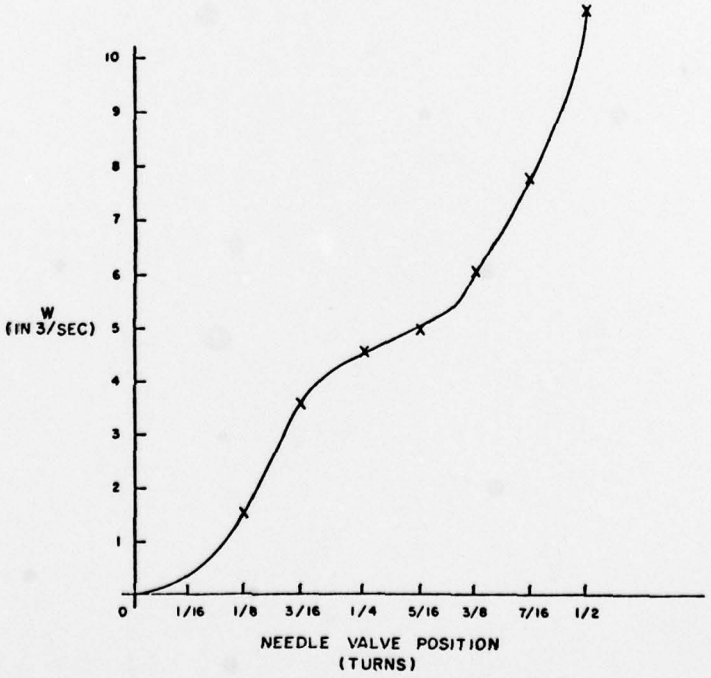

Figure C-2. **Needle valve flow vs turns.**

The pump rate for the ASPT g-seat compressor at cutoff pressure is around 277 in^3/sec (volume of air at atmospheric pressure). Thirty-two needle valves at 5/16 turns open produces a flow of 160 in^3/sec from 6 psig. It has been found from experience that for active flight simulation, the maximum flow rate allowable out of each of the 32 bleed valves, one for each cell, is about 5 in^3/sec, which corresponds to a 5/16 turn setting. The valves cannot be opened wider since the compressor will fall behind in supplying air to the system.

Needle Valve Flow Data

Needle Valve Position	T (seconds)	W (in^3/sec)[a]
1/8	35	1.56
3/16	15	3.63
1/4	12	4.54
5/16	11	4.95
3/8	9	6.05
7/16	7	7.78
1/2	5	10.90

[a]The volumetric flow is assumed to be measured at one atmosphere although this will introduce a small error.

★U.S. GOVERNMENT PRINTING OFFICE:1979- 671-056/42